Journal of the Iranian Chemical Society
https://doi.org/10.1007/s13738-022-02619-3

ORIGINAL PAPER

# Catalytic hydration of terminal alkynes and nitriles without reducing reagents, acidic promoters, and organic solvent over $Fe_3O_4$@Starch–Au

**Seyed Ali Mousavi-Mashhadi**[1] · **Ali Shiri**[1]

Received: 14 April 2022 / Accepted: 2 July 2022


## Abstract

Magnetic heterogeneous nanoparticles ($Fe_3O_4$ NPs) were prepared and functionalized by starch and gold nanoparticles, respectively. The characterization of nanocomposite was carried out by several techniques such as FT-IR, XRD, FE-SEM, TEM, EDS, VSM, ICP, and TGA. The prepared nanocatalyst, $Fe_3O_4$@Starch–Au, was utilized in the synthesis of aryl methyl ketones and amides via the activation of multiple bonds in aqueous media. The nanocatalyst was simply recovered and reused for several cycles without significant loss of its catalytic activity.

## Graphical abstract

Green and environmentally friendly method. Precious catalyst that can recover without difficulty and reused for several times. Safer chemical. Safer solvent. Energy-time efficient. 18 Derivatives

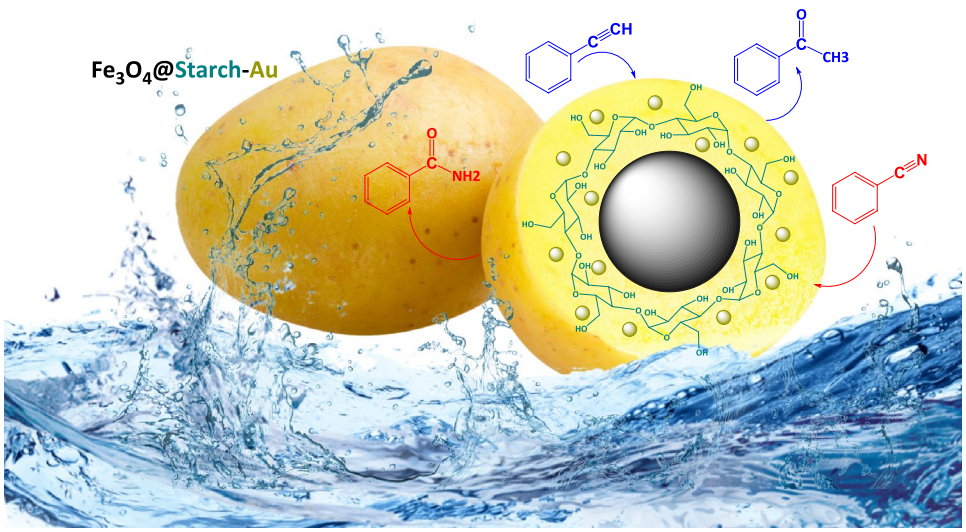


**Keywords** Starch · Alkynes · Nitriles · Aryl methyl ketones · Amides · Magnetic catalyst

## Introduction

Polymers are relevant to various buildings and structures consisting of different compositions and functional groups used as supporting substances in heterogeneous catalytic systems, due to the interaction with metallic ions and nanoparticles [1–8]. Furthermore, natural polysaccharide polymers are attracted in consideration in academic and

✉ Ali Shiri
alishiri@um.ac.ir

[1] Department of Chemistry, Faculty of Science, Ferdowsi University of Mashhad, Mashhad, Iran

Published online: 29 July 2022

industrial research, because of their availability, environmentally and economically characteristics, inexpensive, non-toxic, and eco-friendly attributes [9, 10]. These properties make them excellent candidates for being well-designed and applicable as a support material in catalytic systems [11].

Nowadays, starch is an important and interesting material for the industries due to its large availability and low cost [12]. Starch is a valuable natural polysaccharide and a well-known biopolymer in theoretical and experimental researches. Starch and its derivatives have been recently developed to be one of the excellent materials, due to its distinctive, economic, and remarkable properties. It is a soft and colorless compound which acts as an additive, stabilizer, emulsifier, energy supplement, ethanol fuel, bioplastics, and can be manufactured from the green plants [13]. Starch is one of the greatest biodegradable and sustainable carbohydrates consisting of a large number of glucose units and free hydroxyl groups in the structure, which is capable of chelating to metal ions and particles and can be reestablished from a photosynthesis reaction in plants [14, 15].

Heterogeneous solid supported catalysts due to the easier workup, simplicity of work, and long service life have expanded considerably in modern chemistry [16]. The regular catalytic systems were prepared by immobilization of metal ions onto various solid supports such as magnetic nanoparticles [17–19], zeolite [20–22], metal–organic frameworks (MOFs) [23–27], silica [28–30], mesoporous [31–33], and polymers [34–37], as well as application in producing artificial substances in medical, chemical, engineering, and biochemical reactions. In these procedures, the catalysts can be separated from the reaction medium by simple and efficient methods. Developing magnetic nanoparticles create more convenience in comparison with other catalytic fields because it provides a fast, simple, and more comfortable separation and recovery of the nanocatalyst [6, 38–42].

Along with our previous studies[1, 43–48], we have selected starch as a naturally abandoned, compostable, cheap, and biodegradable compound for the stabilization of gold in it and the application of it in the catalyzed alkynes and nitriles hydration reactions (Scheme 1 and 2).

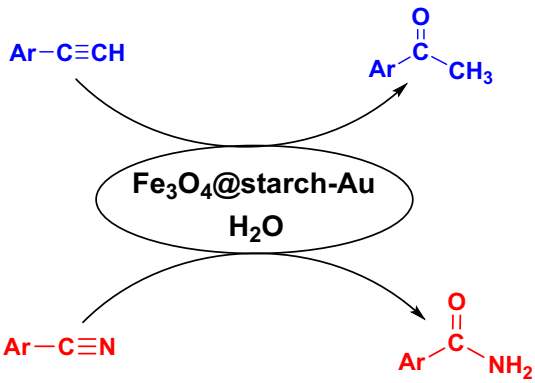


**Scheme 2** Synthesis of aryl methyl ketones and amides by $Fe_3O_4$@Starch–Au

## Experimental section

### Preparation of starch-coated magnetic nanoparticles: $Fe_3O_4$@Starch NPs

Magnetic nanoparticles (MNPs) were prepared by the co-precipitation method. In a typical preparation procedure, $FeCl_3{\cdot}6H_2O$ (1.35 g, 5 mmol) and $FeCl_2{\cdot}4H_2O$ (0.498 g, 2.5 mmol) were dissolved in deionized water (100 mL) under the nitrogen atmosphere with mechanical stirrer at 75 °C. The pH value of the solution was adjusted slowly in 10–11 by aqueous $NH_3$ (25%). The resulting mixture was stirred for another 5 h. The magnetite $Fe_3O_4$ NPs were precipitated out and collected by an external magnet and subsequently washed with ethanol and deionized water. Finally, the collected MNPs were dried in vacuum at 50 °C.

$Fe_3O_4$ NPs (1.00 g) were dispersed in deionized water (50 mL) by sonication for 30 min. To the suspension, the hot aqueous solution of starch (1 g) was gradually added under ultrasonic agitation, and the mixture was sonicated for approximately 20 min. Then, it is subsequently stirred for another 6 h at 60 °C. The coated $Fe_3O_4$@Starch was separated by an external magnet and washed with ethanol (2 × 20 mL) and deionized water (2 × 20 mL) to remove the impurities. The final obtained material was dried under vacuum at 40 °C.

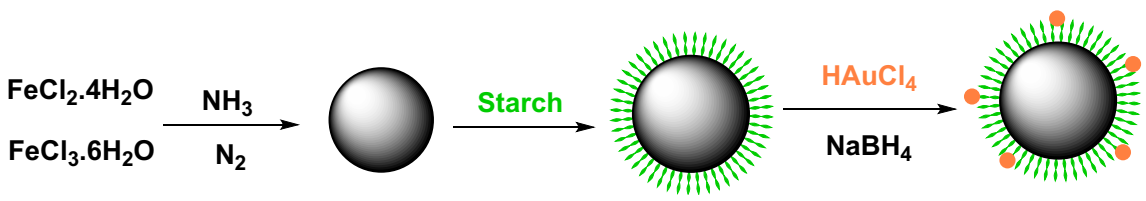


**Scheme 1** Preparation of magnetic nanocomposite $Fe_3O_4$@Starch–Au

## Synthesis of gold nanoparticles coated magnetic starch: $Fe_3O_4$@Starch–Au NPs

$Fe_3O_4$@Starch NPs (500 mg) were ultrasonically dispersed in water (50 mL), then aqueous solution of $HAuCl_4$ (10 mg) in deionized water (50 ml) was added dropwise into the reaction mixture with constant stirring. After being stirred for about 6 h, the excess amount of freshly prepared $NaBH_4$ aqueous solution was slowly added into the dispersion under vigorous stirring at room temperature. The mixture was stirred at this condition for about 5 h. Eventually, $Fe_3O_4$@Starch–Au NPs separated by an external magnet, washed several times with water, and dried under vacuum at 40 °C for overnight.

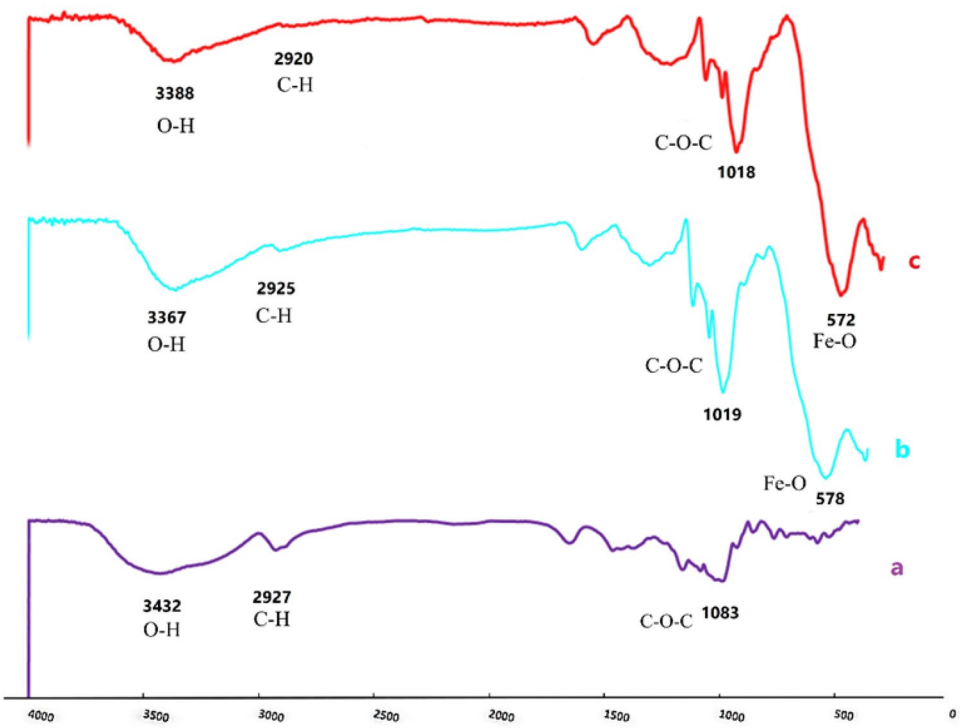


**Fig. 1** Comparison between the FT-IR spectra of **a** starch **b** $Fe_3O_4$@starch **c** $Fe_3O_4$@starch–Au NPs

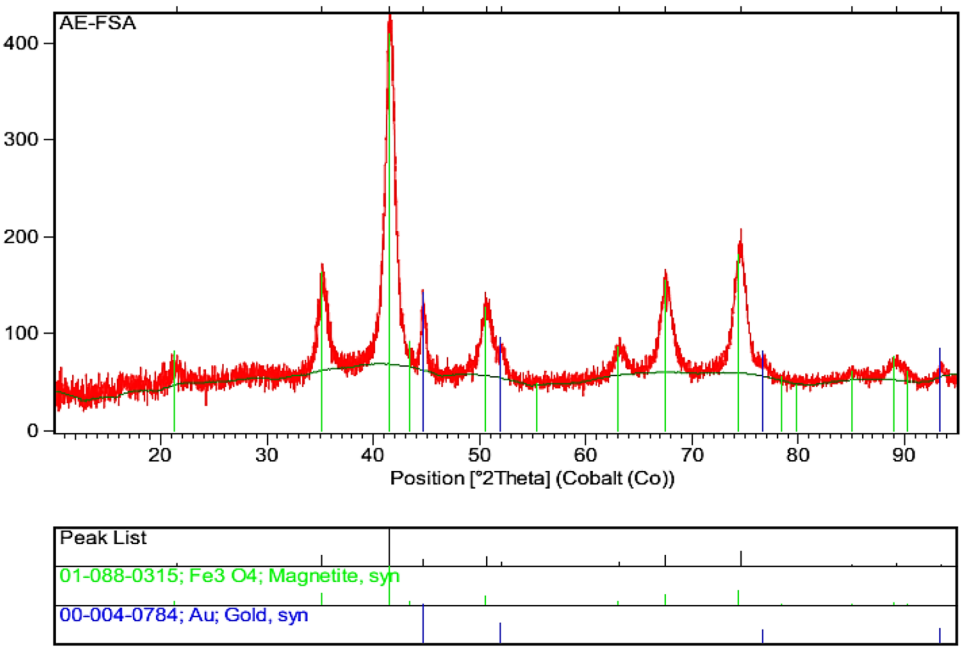


**Fig. 2** XRD pattern of the $Fe_3O_4$@Starch–Au

## General procedure for hydration of terminal alkynes

Alkynes (1 mmol), $H_2O$ (3 mL), and nanocatalyst (20 mg) were added to the flask fitted with a condenser. The reaction mixture was heated in an oil bath at 80 °C. After the completion of the reaction, which was monitored by TLC, the reaction mixture was cooled to room temperature and diluted with ethyl acetate. The catalyst was separated by an external magnet and the organic layer was separated and washed with brine (2 × 20 mL), dried by anhydrous $MgSO_4$, and concentrated under reduced pressure. The residue was purified by column chromatography using silica gel to afford the pure products.

## General procedure for the hydration of nitriles to amides

A mixture of nitrile (1 mmol), water (3 mL) and nanocatalyst (20 mg) was stirred in an oil bath at 80 °C. The progress of the reaction was monitored by TLC until the maximum conversion of nitrile to the corresponding amide occurred. After the completion of the reaction, the mixture was cooled to room temperature and diluted with EtOAc (10 mL). The catalyst was removed by an external magnet, and the mixture was extracted by EtOAc. The organic layer was washed with water (2 × 20 mL) and dried over anhydrous $MgSO_4$. The solvent was evaporated on a rotary evaporator, and the residue was purified by column chromatography.

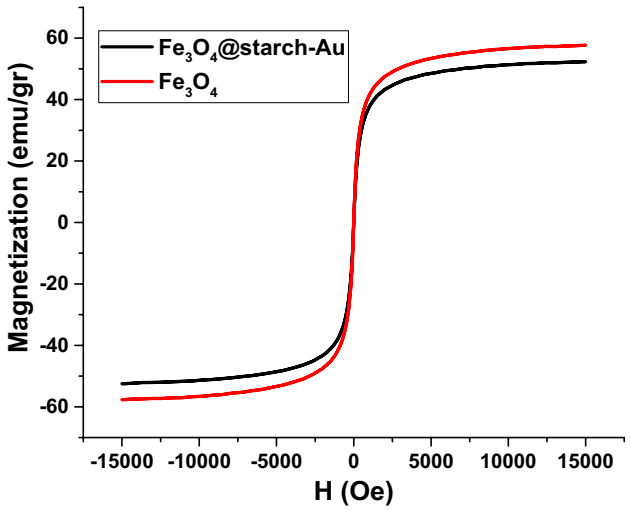


**Fig. 3** Magnetic hysteresis loops of $Fe_3O_4$ nanoparticles and $Fe_3O_4$@Starch–Au nanocomposite

## Results and discussion

The magnetic nanocomposite was prepared and physical and chemical structure of the nanocomposite was evaluated by various techniques such as Fourier transform infrared spectroscopy (FT-IR), X-ray diffraction (XRD), scanning electron microscopy (SEM), transmission electron microscopy (TEM), energy dispersive x-ray (EDX), thermogravimetric analysis (TGA) and vibrating sample magnetometer (VSM).

### FT-IR analysis

FT-IR spectra for starch and starch-coated $Fe_3O_4$ NPs show the characteristic stretching bands in the spectrum of starch at 3432 (O–H), 2927 (C–H), and 1161 (O–C) $cm^{-1}$ (Fig. 1). Moreover, the presence of potent overlapped bands in the 800–1400 $cm^{-1}$ region attributed to the C=O and C–C and C–O bands. Meanwhile, several bands below 800 $cm^{-1}$ correspond to the ring modes. The presence of OH bending vibration in starch appeared at 1621 $cm^{-1}$. The peaks attributed to the stretching vibration of Fe–O bond were overlapped with the starch peaks at wavelength of 576 $cm^{-1}$. The present system exhibits similar functional groups as starch but an increase in the intensities indicated the interaction between

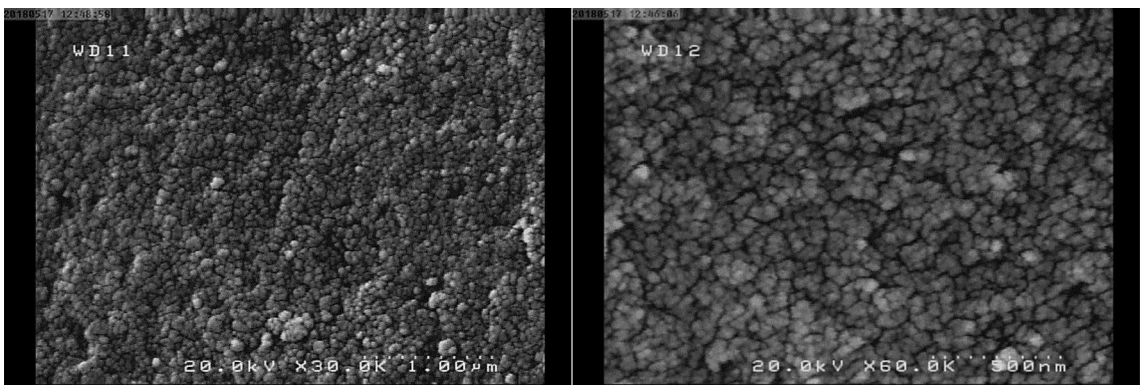


**Fig. 4** SEM images of $Fe_3O_4$@Starch–Au

starch and iron oxide NPs. On the other hand, the shift in the band position can be attributed to the interaction between $Fe_3O_4$ NPs and starch and confirmed that the occurrence of coating of the surface of $Fe_3O_4$ nanoparticles with starch.

## X-ray diffraction (XRD) analysis

In order to confirm the phase structure and crystallinity of the $Fe_3O_4$@Starch–Au nanoparticles, the sample was characterized using XRD analysis (**Fig. 2**). The result verifies the presence of Au nanoparticles on the $Fe_3O_4$@Starch surface with characteristic peaks at $2\theta$ of 35.2°, 41.5°, 50.7°, 63.2°, 67.4°, and 74.6° corresponding to (220), (311), (400), (422), (511), and (440), respectively. The broad reflection peak of the XRD pattern indicates that the starch layer covers successfully on the surface of $Fe_3O_4$ NPs. This observation confirms the presence of Au on the surface of polymeric magnetic particles. According to the XRD reference patterns [01-088-0315] $Fe_3O_4$ iron oxide, [00-004-0784] Au, the catalyst diagrams correspond to the $Fe_3O_4$, and Au peaks, so that it can be deduced the correct synthesis of the nanocatalyst.

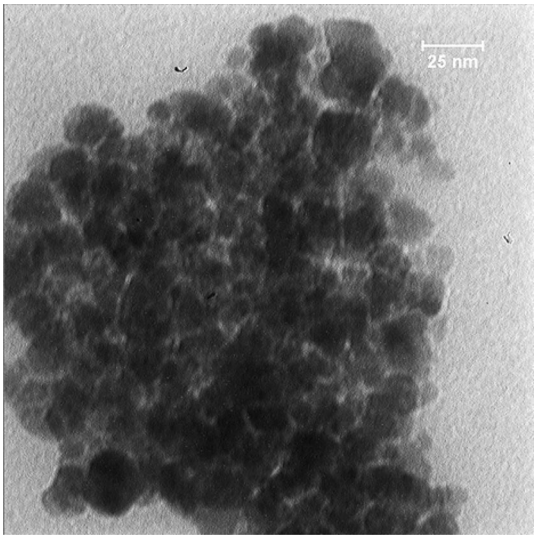


**Fig. 5** TEM image of $Fe_3O_4$@Starch–Au

## Magnetic properties

The magnetic properties of the $Fe_3O_4$ and $Fe_3O_4$@Starch–Au catalyst were performed at room temperature using a vibrating sample magnetometer. The magnetization curves of the samples display no hysteresis loop, which reveals its superparamagnetic characteristics. The saturation magnetization of the magnetic nanoparticles and magnetic nanocomposite were found to be 58 emu $g^{-1}$ and 52 emu $g^{-1}$, respectively. The decrease significantly in saturation magnetization of the nanocomposite was due to the incorporation of the starch in the polymer-coated magnetite. The saturation magnetization value of 52 emu $g^{-1}$ was enough for magnetic separation using an ordinary

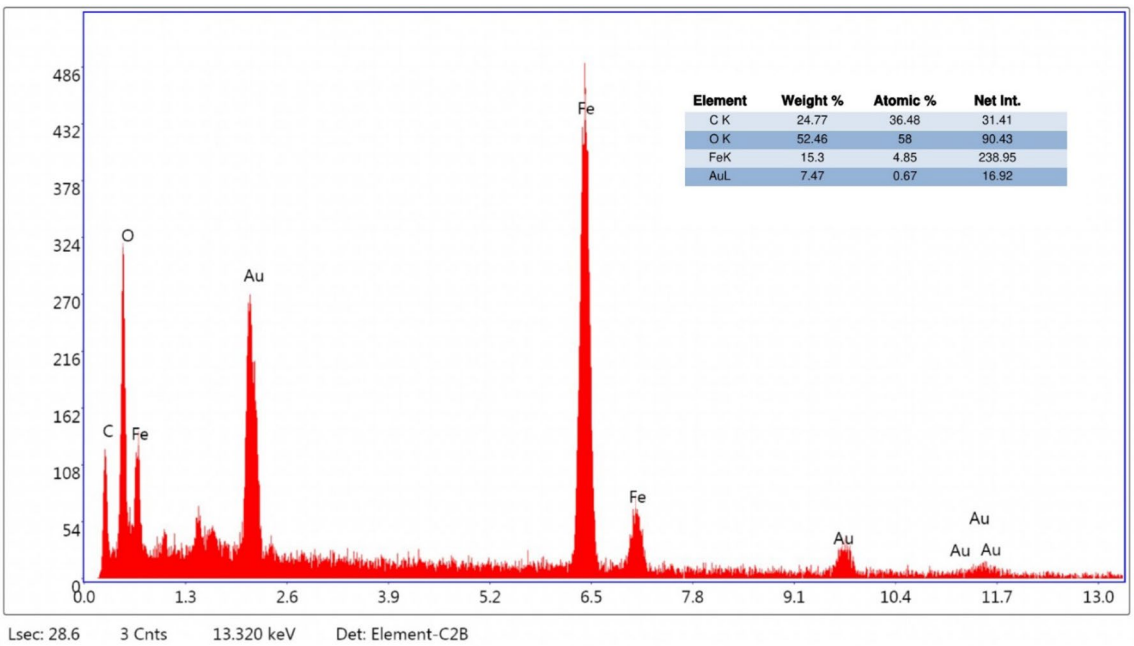


**Fig. 6** EDX spectrum of $Fe_3O_4$@Starch–Au

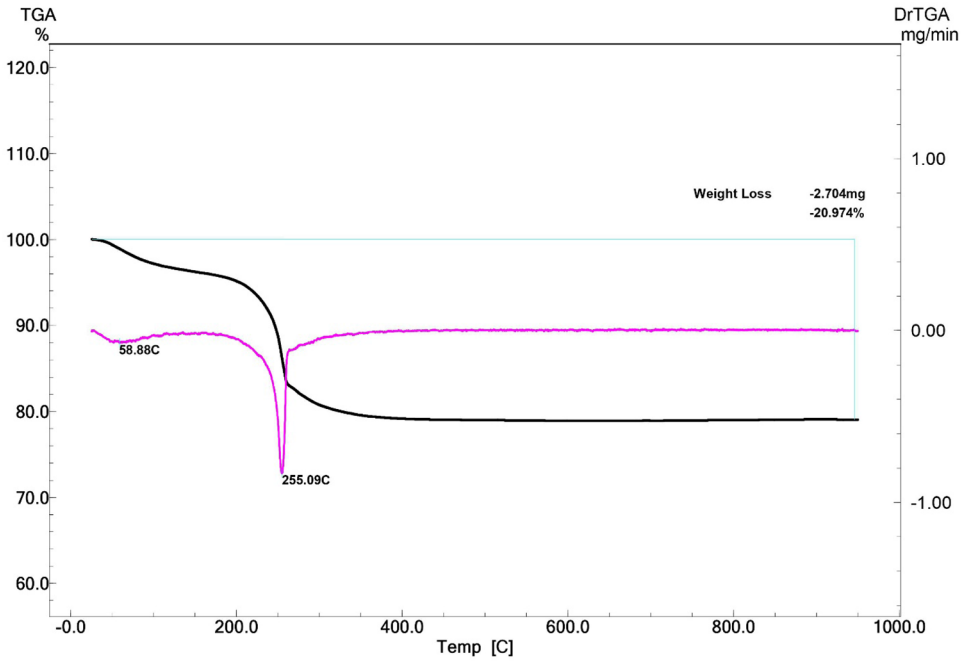


**Fig. 7** TGA curves of $Fe_3O_4$@Starch–Au

magnet. Thus, the magnetization values achieved with the $Fe_3O_4$ content of the starches were sufficient for magnetic separation (Fig. 3).

## Scanning electron microscopy (SEM)

The morphology of the nanocomposite was examined to confirm the shape of the prepared sample using scanning electron microscopy (SEM). The SEM images of $Fe_3O_4$@Starch–Au show the nanocomposite was approximately spherical in morphology with some degree of agglomeration, probably due to the magnetic nature of the nanocatalyst (Fig. 4). This particle size causes further contacts of the catalyst with the reactants, which leads to good yield of the desired product.

| | Au. |
|---|---|
| Conc 1 | 0.954[%] |
| Conc 2 | 0.941[%] |
| *Conc MinRange* | --- |
| **Conc Mean** | **0.947[%]** |
| *Conc MaxRange* | --- |
| **Reported** | **0.947[%]** |

**Fig. 8** ICP analysis of $Fe_3O_4$@Starch–Au NPs

## Transmission electron microscopy (TEM)

The transmission electron microscopy (TEM) image of $Fe_3O_4$@Starch–Au shows an obvious core–shell morphology that the magnetic nanoparticles were covered by the starch shells. TEM discloses the well-defined nanoparticles that were homogeneously distributed in the nanocomposite (Fig. 5).

**Table 1** Optimization of the reaction conditions for the synthesis of aryl methyl ketones

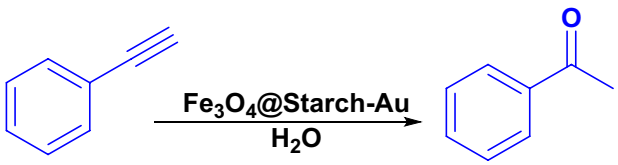


| Entry | Catalyst | Time (h) | Temp. (°C) | Yield (%) |
|---|---|---|---|---|
| 1 | 5 | 6 | 25 | – |
| 2 | 5 | 6 | 50 | > 5 |
| 3 | 5 | 7 | 80 | > 10 |
| 4 | 10 | 6 | 80 | 21 |
| 5 | 10 | 6 | Reflux | 34 |
| 6 | 10 | 7 | Reflux | 43 |
| 7 | 15 | 6 | Reflux | 73 |
| 8 | 20 | 6 | 80 | 80 |
| 9 | **20** | **6** | **80** | **95** |
| 10 | 20 | 7 | Reflux | 95 |
| 11 | – | 7 | Reflux | – |

Reaction conditions: phenylacetylene (1 mmol), water (3 ml).

## Energy-dispersive X-ray analysis of elements (EDX)

EDX analysis of $Fe_3O_4$@Starch–Au shows the presence of C, O, Fe, and Au which provides further evidence for the presence of the gold in the preparation of $Fe_3O_4$@Starch–Au (Fig. 6).

## Thermogravimetric analysis (TGA)

Thermogravimetric analysis was performed for thermal stability, recyclability, and organic content. TGA and DTA with heating the sample in the interval range from 0 to 900 °C demonstrated weight losses peaks around 75–150, and 180–280 °C, which could be attributed to the evaporation

**Table 2** Synthesis of aryl methyl ketones in the presence of $Fe_3O_4$@Starch–Au

| Entry | Alkyne | Product | TON | TOF ($h^{-1}$) | Yield (%) |
|---|---|---|---|---|---|
| 2a | 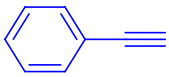 | 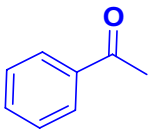 | 4.75 | 0.79 | 95 |
| 2b | 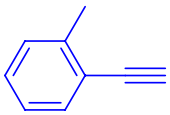 | 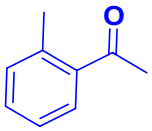 | 4.35 | 0.72 | 87 |
| 2c | 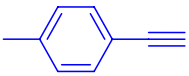 | 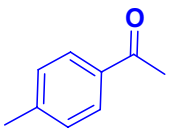 | 4.7 | 0.78 | 94 |
| 2d | 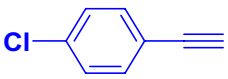 | 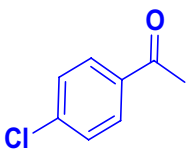 | 4.55 | 0.75 | 91 |
| 2e | 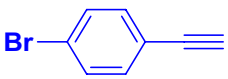 | 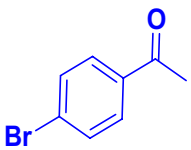 | 4.7 | 0.78 | 94 |
| 2f | 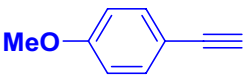 | 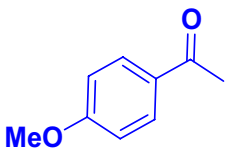 | 4.65 | 0.775 | 93 |
| 2 g | 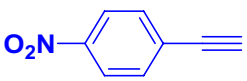 | 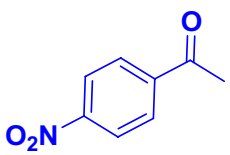 | 4.5 | 0.75 | 90 |
| 2 h | 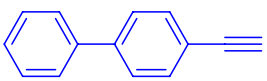 | 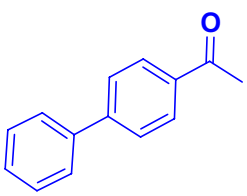 | 4.5 | 0.75 | 90 |

Reaction conditions: Alkyne (1 mmol), catalyst (20 mg), $H_2O$ (3 ml), 80 °C, 6 h

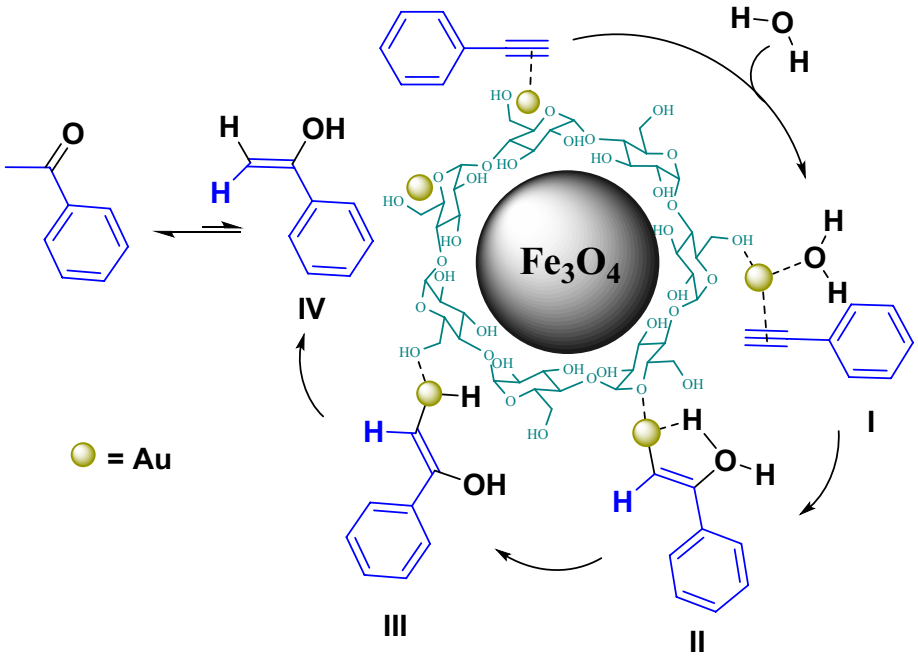


**Scheme 3** A plausible mechanism for the catalytic hydration of terminal alkynes over $Fe_3O_4$@Starch–Au

of the remaining water, and starch over magnetic nanoparticles decomposition (Fig. 7). It is demonstrated that the most of the weight of the prepared catalyst be related to $Fe_3O_4$ as the mineral part.

The gold content of the nanocomposite, as determined by ICP, was obtained to be 0.947% that confirmed the presence of Au species in the structure of the nanocomposite (Fig. 8).

## Catalytic application of $Fe_3O_4$@Starch–Au catalyst

To optimize the reaction condition, phenylacetylene (Table 1) and benzonitrile (Table 3) were chosen as the model substrates for alkynes and nitriles hydration in the presence of $Fe_3O_4$@Starch–Au, respectively. The effect of catalyst amounts weas investigated through the variation of the catalyst amount in the range of 5 to 20 mg. Gradual improvements in yields were observed in 20 mg of the nanocatalyst, and further increasing of the catalyst amount did not have accountable result on the yield. In the absence of the catalyst, no hydration was observed, thus it confirms the role of the catalyst in the occurrence of the reaction. The reactions were remarkably accelerated by increasing the reaction temperature from room temperature to 100 °C. The temperature at 80 ºC was selected as the optimum temperature because the yields improved progressively from 0 to 95% for phenylacetylene (Table 1) and from 0 to 93% for benzonitrile (Table 3).

To study the synthetic efficiency of the nanocatalyst, the substrate scopes of this methodology were investigated

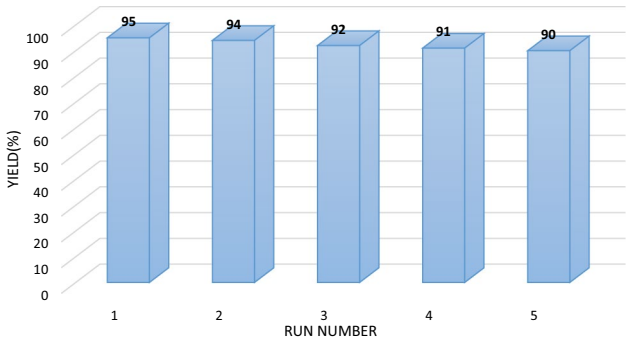


**Fig. 9** Recycling activity of the $Fe_3O_4$@Starch–Au nanocatalyst in the synthesis of aryl methyl ketones

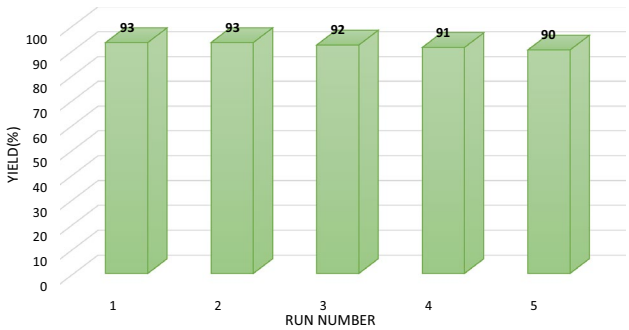


**Fig. 10** Recycling activity of the $Fe_3O_4$@Starch–Au nanocatalyst in the synthesis of amides

**Table 3** Optimization of the reaction conditions for the synthesis of amides

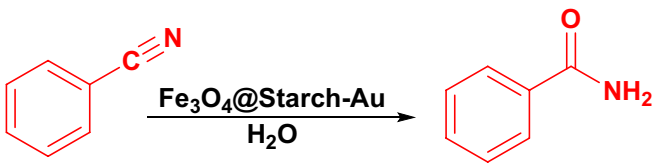


| Entry | Catalyst | Time (h) | Temp. (°C) | Yield (%) |
|---|---|---|---|---|
| 1 | 5 | 5 | 25 | – |
| 2 | 5 | 5 | 50 | Trace |
| 3 | 5 | 5 | 80 | 15 |
| 4 | 10 | 4 | 80 | 28 |
| 5 | 10 | 4 | Reflux | 35 |
| 6 | 15 | 4 | 80 | 68 |
| 7 | 15 | 4 | Reflux | 78 |
| 8 | **20** | **4** | **80** | **93** |
| 9 | 20 | 4 | Reflux | 93 |
| 10 | – | 5 | Reflux | – |

Reaction conditions: benzonitrile (1 mmol), water (3 ml)

under the optimized reaction conditions. A series of aromatic alkynes and nitriles with different substituent groups on the phenyl ring was exposed to this hydration process. All the substrates were efficiently converted into the corresponding ketones (Table 2) and amides (Table 4) in good to excellent yields.

Initially, the addition of Au onto phenylacetylene resulted in alkyne activation. This is reliable with catalytic evaluations that display coordinative Au sites at metal-support interfaces, which increase activity bonds in alkynes. Subsequent addition of $H_2O$ to the surface of the catalyst and attacks to form II. Dissociation of protons from water along with association at carbon occurs to form the intermediate III, and the resulting enol intermediate was formed the intermediate IV. Further rearrangements of the enol intermediate produce the final products and simply remove the catalyst surface. The catalyst goes back to the catalytic cycle to continue another reaction cycle (Scheme 3).

The possibility of recycling and recovery of the prepared nanocatalyst through simple and physical processes and their stability during the reaction are two imperative issues from the operation viewpoints. Therefore, the development of more practical procedures for catalyst recovery is still a very attractive issue. Using this proper recycling process, the nanocatalyst system can be recovered at least five times without significant loss of its performance (Figs. 9, 10).

As it is presented in Tables 3 and 4, the comparison of this catalyst with some recently published catalysts has been performed. Various conditions have been applied, but the use of green and nontoxic reaction conditions has not been reported. Employing reachable and no harmful materials, achieving high yields of product, and mild reaction condition is the art of this study (Tables 5 and 6).

## Conclusions

We have successfully demonstrated a magnetic $Fe_3O_4$@Starch–Au nanocatalyst as a convenient and effective method that catalyzed the hydration of various terminal alkynes and nitriles to methyl ketones and amides, respectively. We consider that the use of easily available, nonhazardous, and reusable $Fe_3O_4$@Starch–Au as a nanocatalyst makes this procedure practical. Notable advantages offered by this research are the absence of reducing reagents and organic solvent, with a broad substrate scope. Higher yields of the series of methyl ketones and amides, operationally simple procedure, and mild reaction conditions, which make them an attractive and useful alternative to the existing methods. Remarkably, this investigation exhibited the potential of the direct use of nanocatalyst for the activation of multiple bonds for organic synthesis. The magnetically recyclable nanocatalyst can be recovered from the reaction mixture and reused in subsequent runs

**Table 4** Synthesis of amides in the presence of $Fe_3O_4$@Starch–Au

| Entry | Nitrile | Amide | TON | TOF($h^{-1}$) | Yield (%) |
|---|---|---|---|---|---|
| 4a | 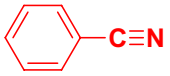 | 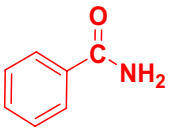 | 4.65 | 1.16 | 93 |
| 4b | 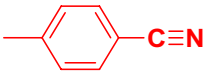 | 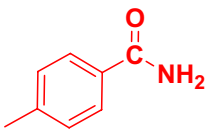 | 4.6 | 1.15 | 92 |
| 4c | 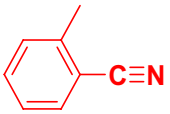 | 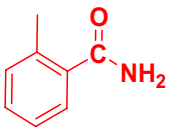 | 4.3 | 1.08 | 86 |
| 4d | 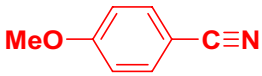 | 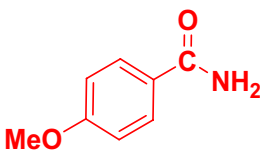 | 4.55 | 1.13 | 91 |
| 4e | 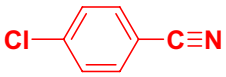 | 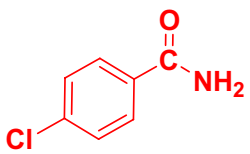 | 4.5 | 1.12 | 90 |
| 4f | 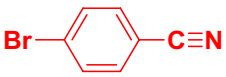 | 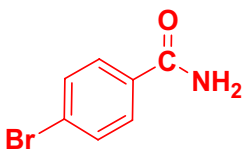 | 4.65 | 1.16 | 93 |
| 4 g | 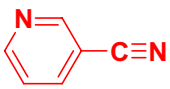 | 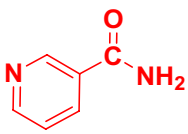 | 4.5 | 1.12 | 90 |
| 4 h | 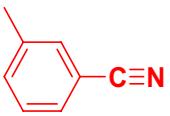 | 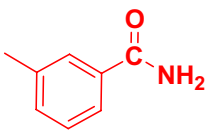 | 4.5 | 1.12 | 90 |
| 4i | 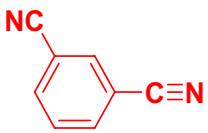 | 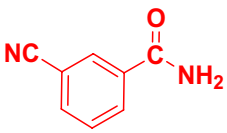 | 4.6 | 1.15 | 92 |
| 4j | 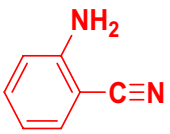 |  | 4.25 | 1.06 | 85 |

Reaction conditions: nitrile (1 mmol), catalyst (20 mg), $H_2O$ (3 ml), 80 °C, 4 h

**Table 5** Comparison of catalytic activity of the $Fe_3O_4$@Starch–Au synthesis of aryl methyl ketones

| Entry | Condition | Time (h) | Yield (%) | Ref |
|---|---|---|---|---|
| 1 | Different Au(I,III)complexes, $H_2SO_4$, $H_2O$ at 75 °C | 5 | 79 | [49] |
| 2 | CuCl, HCl(aq), MeOH at 90 °C | 6 | 90 | [50] |
| 3 | Salen–gold(III) complex,$CF_3COOH$,MeOH at 80 °C | 5 | 93 | [51] |
| 4 | Salen-Co(III) complex, $H_2SO_4$,$CH_3OH$ at 80 °C | 20 | 91 | [52] |
| 5 | $Fe_3O_4$@Starch–Au,$H_2O$ at 80 °C | 6 | 95 | Current Work |

**Table 6** Comparison of catalytic activity of the $Fe_3O_4$@Starch–Au NPs synthesis of amides

| Entry | Condition | Time (h) | Yield (%) | Ref |
|---|---|---|---|---|
| 1 | 25PdMPAV1/$TiO_2$, water at 140 °C | 6 | 88 | [53] |
| 2 | Half-sandwich ruthenium, IPA at 80 °C | 4 | 92 | [54] |
| 3 | Ru/chitin, $H_2O$, $N_2$ atmosphere at 120 °C | 20 | 87 | [55] |
| 4 | Complexes of palladium(II), $H_2O$-THF at 80 °C | 5 | 95 | [56] |
| 5 | $Fe_3O_4$@Starch–Au,$H_2O$ at 80 °C | 4 | 93 | Current Work |

without the observation of significant decrease in activity even after five runs. These magnetic nanocomposites are highly efficient and stable heterogeneous catalysts for nitriles and alkynes hydration reactions in a green approach.

**Supplementary Information** The online version contains supplementary material available at https://doi.org/10.1007/s13738-022-02619-3.

## References


1. S.A. Mousavi Mashhadi, M.Z. Kassaee, E. Eidi, Appl. Organomet. Chem. **33**, 1 (2019)
2. H. Veisi, S. Najafi, S. Hemmati, Int. J. Biol. Macromol. **113**, 186 (2018)
3. L. Liu, A. Corma, Chem. Rev. **118**, 4981 (2018)
4. A. Azizi, J. Inorg. Organomet. Polym. Mater. **30**, 3552 (2020)
5. Z. Naderi, J. Azizian, E. Moniri, N. Farhadyar, J. Inorg. Organomet. Polym. Mater. **30**, 1339 (2020)
6. A. Maleki, M. Kamalzare, M. Aghaei, J. Nanostructure Chem. **5**, 95 (2015)
7. E.G. Lemraski, S. Yari, E.K. Ali, S. Sharafinia, H. Jahangirian, R. Rafiee-Moghaddam, T.J. Webster, J. Iran. Chem. Soc. **19**, 1287 (2022)
8. A. Maleki, V. Eskandarpour, J. Iran. Chem. Soc. **16**, 1459 (2019)
9. A. Maleki, A.A. Jafari, S. Yousefi, J. Iran. Chem. Soc. **14**, 1801 (2017)
10. A. Maleki, M. Aghaei, R. Paydar, J. Iran. Chem. Soc. **14**, 485 (2017)
11. X. Wang, P. Hu, F. Xue, Y. Wei, Carbohydr. Polym. **114**, 476 (2014)
12. F.A. Aouada, L.H.C. Mattoso, E. Longo, Ind. Crops Prod. **50**, 449 (2013)
13. M.A. Araújo, A.M. Cunha, M. Mota, Biomaterials **25**, 2687 (2004)
14. M. Gholinejad, N. Jeddi, A.C.S. Sustain, Chem. Eng. **2**, 2658 (2014)
15. R. Bonyasi, M. Gholinejad, F. Saadati, C. Nájera, New J. Chem. **42**, 3078 (2018)
16. F. Zaera, Chem. Soc. Rev. **42**, 2746 (2013)
17. B. Karimi, F. Mansouri, H.M. Mirzaei, ChemCatChem **7**, 1736 (2015)
18. T. Zeng, W.-W. Chen, C.M. Cirtiu, A. Moores, G. Song, C.-J. Li, Green Chem. **12**, 570 (2010)
19. A. Rashidi Vahid, F. Hajishaabanha, S. Shaabani, H. Farhid, A. Shaabani, J. Iran. Chem. Soc. **19**, 2601–2615 (2022)
20. Y. Li, L. Li, J. Yu, Chem **3**, 928 (2017)
21. T. Rashid, D. Iqbal, A. Hazafa, S. Hussain, F. Sher, F. Sher, J. Environ. Chem. Eng. **8**, 104023 (2020)
22. A. Hajipour, F. Derakhshanfard, A. Mehrizad, L. Amirkhani, J. Inorg. Organomet. Polym. Mater. **31**, 2714 (2021)
23. A.H. Chughtai, N. Ahmad, H.A. Younus, A. Laypkov, F. Verpoort, Chem. Soc. Rev. **44**, 6804 (2015)
24. J. Park, J.-R. Li, Y.-P. Chen, J. Yu, A.A. Yakovenko, Z.U. Wang, L.-B. Sun, P.B. Balbuena, H.-C. Zhou, Chem. Commun. **48**, 9995 (2012)
25. Z. Ghiamaty, A. Ghaffarinejad, M. Faryadras, A. Abdolmaleki, H. Kazemi, J. Nanostructure Chem. **6**, 299 (2016)
26. S.N. Nangare, S.R. Patil, A.G. Patil, Z.G. Khan, P.K. Deshmukh, R.S. Tade, M.R. Mahajan, S.B. Bari, P.O. Patil, J. Nanostructure Chem. (2021). https://doi.org/10.1007/s40097-021-00449-y
27. Z. Gharehdaghi, R. Rahimi, S.M. Naghib, F. Molaabasi, J. Iran. Chem. Soc. **19**, 2727–2737 (2022)
28. J. Liang, Z. Liang, R. Zou, Y. Zhao, Adv. Mater. **29**, 1701139 (2017)
29. T. Shamim, S. Paul, Catal. Lett. **136**, 260 (2010)
30. A. Maleki, R. Rahimi, S. Maleki, J. Nanostructure Chem. **4**, 153 (2014)
31. N. Salam, S.K. Kundu, A.S. Roy, P. Mondal, S. Roy, A. Bhaumik, S.M. Islam, Catal. Sci. Technol. **3**, 3303 (2013)
32. B. Dutta, S. March, L. Achola, S. Sahoo, J. He, A.S. Amin, Y. Wu, S. Poges, S.P. Alpay, S.L. Suib, Green Chem. **20**, 3180 (2018)
33. A. Maleki, Z. Hajizadeh, P. Salehi, Sci. Rep. **9**, 1 (2019)
34. S. Basaveni, N.V. Kuchkina, Z.B. Shifrina, M. Pal, M. Rajadurai, J. Nanoparticle Res. **21**, 1 (2019)
35. M.S. Khalili, K. Zare, O. Moradi, M. Sillanpää, J. Nanostructure Chem. **8**, 103 (2018)
36. P. Kamalzare, B. Mirza, S. Soleimani-Amiri, J. Nanostructure Chem. **11**, 229 (2021)
37. A. Maleki, M. Ghassemi, R. Firouzi-Haji, Pure Appl. Chem. **90**, 387 (2018)
38. C.W. Lim, I.S. Lee, Nano Today **5**, 412 (2010)

39. S. Shylesh, V. Schünemann, W.R. Thiel, Angew. Chemie Int. Ed. **49**, 3428 (2010)
40. W. Wu, Z. Wu, T. Yu, C. Jiang, W.S. Kim, Sci. Technol. Adv. Mater. **16**, 1–43 (2015)
41. A. Khorshidi, S. Ansari, S. Shariati, J. Iran. Chem. Soc. **19**, 3473–3480 (2022)
42. A. Bovand, H. Kargar, M. Fallah-Mehrjardi, J. Iran. Chem. Soc. **19**, 3463–3471 (2022)
43. S.A. Mousavi-Mashhadi, A. Shiri, ChemistrySelect **6**, 3941 (2021)
44. K. Hoseinzade, S.A. Mousavi-Mashhadi, A. Shiri, J. Inorg. Organomet. Polym. Mater. **31**, 4648 (2021)
45. Z. Ghadamyari, A. Shiri, A. Khojastehnezhad, S.M. Seyedi, Appl. Organomet. Chem. **33**, 1 (2019)
46. M. Keyhaniyan, A. Shiri, H. Eshghi, A. Khojastehnezhad, Appl. Organomet. Chem. **32**, 1 (2018)
47. M. Keyhaniyan, A. Shiri, H. Eshghi, A. Khojastehnezhad, New J. Chem. **42**, 19433 (2018)
48. K. Hoseinzade, S.A. Mousavi-Mashhadi, A. Shiri, Mol. Divers. (2022). https://doi.org/10.1007/s11030-021-10368-3
49. X. Wang, Y. Wang, J. Zhang, X. Zhao, Y. Liu, J. Organomet. Chem. **762**, 40 (2014)
50. T.F. Niu, D.Y. Jiang, S.Y. Li, X.G. Shu, H. Li, A.L. Zhang, J.Y. Xu, B.Q. Ni, Tetrahedron Lett. **58**, 1156 (2017)
51. T. Chen, C. Cai, Catal. Commun. **65**, 102 (2015)
52. S. Wang, C. Miao, W. Wang, Z. Lei, W. Sun, Cuihua Xuebao/ Chinese. J. Catal. **35**, 1695 (2014)
53. B. Srinivasa Rao, A. Srivani, D. Dhana Lakshmi, N. Lingaiah, Catal. Lett. **146**(10), 2025–2031 (2016). https://doi.org/10.1007/s10562-016-1816-4
54. W.G. Jia, S. Ling, S.J. Fang, E.H. Sheng, Polyhedron **138**, 1 (2017)
55. A. Matsuoka, T. Isogawa, Y. Morioka, B.R. Knappett, A.E.H. Wheatley, S. Saito, H. Naka, RSC Adv. **5**, 12152 (2015)
56. P. Dubey, S. Gupta, A.K. Singh, Dalt. Trans. **46**, 13065 (2017)